Published online 4 January 2010

Nucleic Acids Research, 2010, Vol. 38, No. 6 ***1889–1901***
doi:10.1093/nar/gkp1199

Mph1 requires mismatch repair-independent and -dependent functions of MutSα to regulate crossover formation during homologous recombination repair

Ye Dee Tay, Julie M. Sidebotham and Leonard Wu*

Weatherall Institute of Molecular Medicine, University of Oxford, John Radcliffe Hospital, Headington Oxford, OX3 9DS, UK

Received October 1, 2009; Revised November 17, 2009; Accepted December 9, 2009

ABSTRACT

In budding yeast the DNA helicase Mph1 prevents genome rearrangements during ectopic homologous recombination (HR) by suppressing the formation of crossovers (COs). Here we show that during ectopic HR repair, the anti-CO function of Mph1 is intricately associated with the mismatch repair (MMR) factor, MutSα. In particular, during HR repair using a completely homologous substrate, we reveal an MMR-independent function of MutSα in generating COs that is specifically antagonized by Mph1, but not Sgs1. In contrast, both Mph1 and MutSα are required to efficiently suppress COs in the presence of a homeologous substrate. Mph1 acts redundantly with Sgs1 in this respect since *mph1Δ sgs1Δ* double mutant cells pheno-copy MutSα mutants and completely fail to discriminate homologous and homeologous sequences during HR repair. However, this defect of *mph1Δ sgs1Δ* cells is not due to an inability to carry out MMR but rather is accompanied by elevated levels of gene conversion (GC) and bi-directional GC tracts specifically in non-crossover products. Models describing how Mph1, MutSα and Sgs1 act in concert to suppress genome rearrangements during ectopic HR repair are discussed.

INTRODUCTION

Homologous recombination (HR) is a multi-pathway process for the repair of DNA double-strand breaks (DSBs) (Figure 1) (1). In nearly all pathways of HR, a 3′ tail generated from the resection of a DNA end undergoes Rad51-mediated strand exchange with a homologous donor molecule to form a D-loop (1). In the synthesis-dependent strand-annealing (SDSA) pathway of HR, the D-loop is dismantled and the single-stranded ends of the break anneal via limited stretches of DNA repair synthesis (1) (Figure 1). Alternatively, the D-loop can be extended allowing capture of the second end of the break, which, following repair synthesis and ligation to fill in single-stranded gaps, results in the formation of a double Holliday junction (HJ) structure. The double HJ structure can then be processed by the dissolution pathway of HR in which convergent branch migration of the two HJs causes them to collapse into a hemicatenane that is then decatenated by topoisomerase III enzymes (2,3). Alternatively, the two HJs may be subjected to the resolution pathway of HR in which each junction is symmetrically cleaved in one of two orientations by HJ resolvases. Distinct outcomes arise through the use of these different HR pathways in that SDSA and dissolution give rise exclusively to non-crossovers (NCOs) whereas resolution can give rise to both NCOs and crossovers (CO) (1,3) (Figure 1).

Recently the budding yeast DNA helicase Mph1 has been shown to suppress COs during the repair of an HO endonuclease-induced genomic DSB (4). Mph1 is a 3′–5′ DNA helicase that has been implicated in HR regulation and the processing of replication intermediates (5–9). It has been proposed that the anti-CO functions of Mph1 are mediated through the ability of Mph1 to disrupt D-loops and thus facilitate SDSA (4). Mph1 acts non-epistatically with two other helicases that also function to suppress CO recombination, Sgs1 and Srs2 (2,4). Srs2 dismantles Rad51 nucleoprotein filaments and is also thought to promote SDSA, whereas Sgs1 has been proposed to be required for double HJ dissolution together with Top3 and Rmi1 (2,10–13).

*To whom correspondence should be addressed. Tel: +44 1865 222414; Fax: +44 1865 222431; Email: Leonard.wu@imm.ox.ac.uk

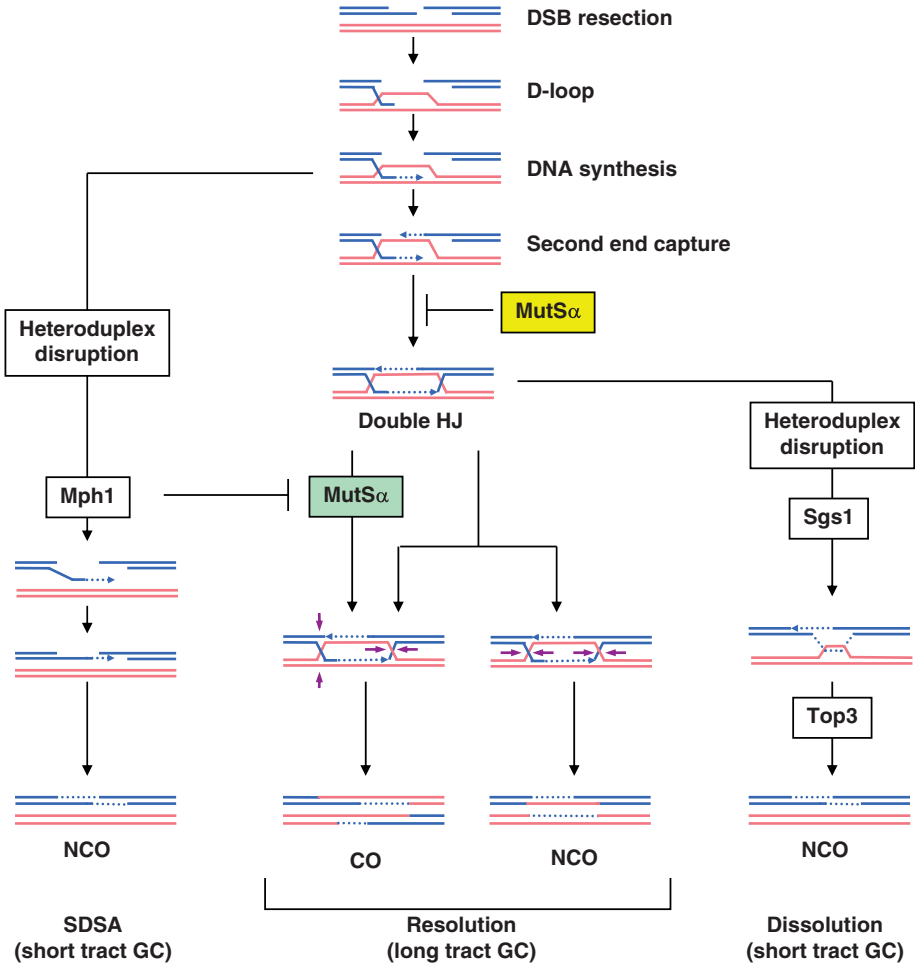

Figure 1. Schematic diagram showing the outcomes of different homologous recombination repair pathways and the proposed steps in which Mph1, MutSα and Sgs1 act. During homeologous recombination repair, MutSα specifically suppresses the formation of COs by inhibiting Double HJ formation (yellow box). However, during homologous recombination, MutSα-dependent COs are generated that do not require the MMR functions of MutSα and are suppressed by the actions of Mph1 (green box). Tracts of DNA synthesis are shown by dotted blue lines with arrowheads. The resolution of HJs in one of two orientations is shown by magenta arrowheads. See text for details.

The suppression of COs is of particular importance during mitotic HR to prevent potentially deleterious genome rearrangements, such as chromosome translocations and loss-of-heterozygosity, if a non-sister is used as the donor sequence for HR repair. Non-sister recombination is likely to involve similar, but non-identical (homeologous) sequences. Heteroduplex DNA generated by Rad51-mediated strand exchange between homeologous sequences will thus contain DNA mismatches. The mismatch repair (MMR) machinery plays key roles in regulating homeologous recombination (14–16). DNA mismatch recognition is effected by MutSα and MutSβ, which in budding yeast comprise heterodimeric complexes of *Escherichia coli* MutS homologues Msh2/Msh6 and Msh2/Msh3, respectively. While MutSα predominantly acts to recognise base–base mismatches, MutSβ recognizes small insertion/deletion loops up to 12 bp in length (17–20). In addition to their role in mismatch recognition during homeologous recombination, Msh2 and Msh3 also function with the heterodimeric nuclease Rad1/Rad10 to remove non-complementary 3′ tails that are >30 nucleotides in length during HR and single-strand annealing (SSA) (21,22,23). All four factors also act epistatically to regulate a subset of COs during HR (24–26).

In this study, we reveal that Mph1 specifically suppresses a subset of COs that are dependent on MutSα but independent of the MMR functions of MutSα. In contrast to this antagonistic interaction between Mph1 and MutSα during HR, we find that *mph1Δ* cells also have a defect in a MutSα-dependent process in which COs are suppressed when a homeologous sequence is used to target repair. This function of Mph1 acts in parallel to the RecQ helicase, Sgs1, since *mph1Δ sgs1Δ* cells pheno-copy MutSα mutants in their inability to discriminate homologous and homeologous sequences during HR repair. Analysis of homeologous recombination repair products from *mph1Δ sgs1Δ* cells does not however indicate an overt defect in MMR in the absence of Mph1 and Sgs1. Rather our results suggest that Mph1, MutSα and Sgs1 act in concert at functionally separable steps to inhibit the formation of double HJs.

MATERIALS AND METHODS

Strains

All strains were generated in a BY4741 background (*Mat a*; *his3Δ1*; *leu2Δ0*; *met15Δ0*; *ura3Δ0*). Single deletion mutants were obtained from the *Saccharomyces cerevisiae* genome deletion collection (Open Biosystems). The *msh2Δ1*, *msh6-340* and *msh6-G987D* alleles were constructed using the Delitto Perfetto methodology to introduce the desired mutations into their respective endogenous loci (27). Briefly, the endogenous *MSH2* or *MSH6* genes were disrupted by insertion of a hygromycin resistance/*URA3* cassette that was amplified by PCR from plasmid pGSHU using primer pairs Msh2PI and Msh2PIIS or Msh6PI and Msh6PIIS, respectively (Supplementary Figure 1). Following isolation and confirmation by PCR analysis of clones with the desired targeting event, excision of the hygromycin resistance/*URA3* cassette to generate *msh2Δ1* was performed by transformation with a duplex HpaI DNA fragment, msh2Δ1IRO, which was synthesized by Genscript (Supplementary Figure S1). Excision of the hygromycin resistance/*URA3* cassettes to generate *msh6-340* and *msh6-G987D* alleles was performed by transformation with IRO duplexes comprising Xho1I fragments derived from plasmids pEAE129 and pEAE216, respectively. Excision events were selected for by growth on 5-FOA. *mph1Δ sgs1Δ*, *mph1Δ msh2Δ*, *mph1Δ mph3Δ*, *mph1Δ sgs1Δ* and *mph1Δ msh2Δ1*strains were constructed by replacing the entire *MPH1* ORF in the respective single mutant with a hygromycin resistant cassette by conventional gene replacement strategies. All strains were confirmed by PCR and sequence analysis of genomic DNA.

Plasmids

pADE2(400/400) was constructed by the following modifications to plasmid pRS401: ARS209 was amplified by PCR using primers A1 and A2 using plasmid pRS412 as a template (for primer sequences see Supplementary Figure S1). The resulting fragment was cloned into pRS401 via AatII sites introduced into the ARS-containing fragment by PCR to generate pRS401/ARS. A fragment containing nucleotides 200–999, of the *S. cerevisiae ADE2* ORF was amplified by PCR using BY4741 genomic DNA as a template and cloned into pRS401/ARS via PCR-introduced BamHI sites to generate pADE2(400/400) (For sequence see Supplementary Figure 2). The homeologous *ADE2* sequence used to generate pADE2(1 bp/mis) was synthesized by Genscript and cloned into pRS401/ARS via Xma1 and Spe1 sites to generate pADE2(1 bp/mis) (for sequence see Supplementary Figure 2). The orientation and sequences of inserts of all clones were confirmed by sequencing. The sequences of the *ADE2*-derived fragments in the plasmids used in this study are shown in Supplementary Figure 2. Plasmids pEAE129 (28) and pEAE216 (29) were kind gifts from Eric Alani. Plasmid pGSHU (27) was a kind gift from Francesca Storici.

Plasmid break repair assay

Repair substrates were linearized by digestion with Hpa1 (New England BioLabs) and gel purified using a Qiagen Gel extraction kit. Cells were transformed with 400 ng cut DNA using the Frozen-EZ yeast transformation II^{TM} kit (Zymo Research) following the manufacturer's recommendations. The cut plasmid was also co-transformed with pYES plasmid to control for variations in inter-sample transformation efficiencies in order to calculate absolute repair efficiencies. Following transformation, cells were plated onto the appropriate media to select for repair events (SD-met) or pYES transformants (SD-ura) and plates were incubated at 30°C for 3 days. In repair assays, transformants arising as red or white colonies were counted and scored as CO and NCO repair events, respectively. Repair assays were performed a minimum of three times.

Analysis of repair products

Cultures (1.5 ml) from individual colonies arising from repair plasmid-break repair assays were grown up in selective media. Cells were pelleted by centrifugation and resuspended in 0.2 ml of 2% Triton X-100, 1% SDS, 0.1 M NaCl, 10 mM Tris–HCl (pH 8), 1 mM EDTA. Phenol:chloroform:isomamyl alcohol (25:24:1) (0.2 ml) was added together with 0.3 g acid-washed glass beads and cells were lysed in a FastPrep FP120 bead beater (Thermo Electron Corporation). DNA in the aqueous phase was ethanol precipitated and rinsed with 70% ethanol before being re-suspended in TE (pH 8). Primer pair N1 and N2 was used to amplify the pADE2(1 bp/mis)-derived *ADE2* sequences from genomic DNA derived from NCO products. Primer pairs C1 and C2, and C3 and C4 were used to amplify fragments from genomic DNA derived from CO products that contained pADE2(1 bp/mis)-derived *ADE2* markers 5–9 and markers 0–4, respectively (for primer sequences see Supplementary Figure S1). PCR products were sequenced to determine the status of each individual marker in each of the individual products.

RESULTS

Mph1 acts to suppress COs during extra-chromosomal recombination

To analyze the role of Mph1 in the regulation of COs during ectopic recombination we utilized a plasmid break repair assay. We opted for a plasmid repair assay because HR-mediated repair of a linearized plasmid transformed into yeast parallels many aspects of the repair of a single genomic DSB as both processes require and are modulated by many of the same genetic factors (1,2,30–33). Moreover, plasmid break repair assays readily allow us to alter the sequence of the repair substrate and to score and analyze individual repair events. Plasmid pADE2(400/400) contains an 800 bp fragment corresponding to residues 200–999 of the *ADE2* ORF in *S. cerevisiae*, the *MET15* auxotrophic marker and a yeast autonomous replicating sequence

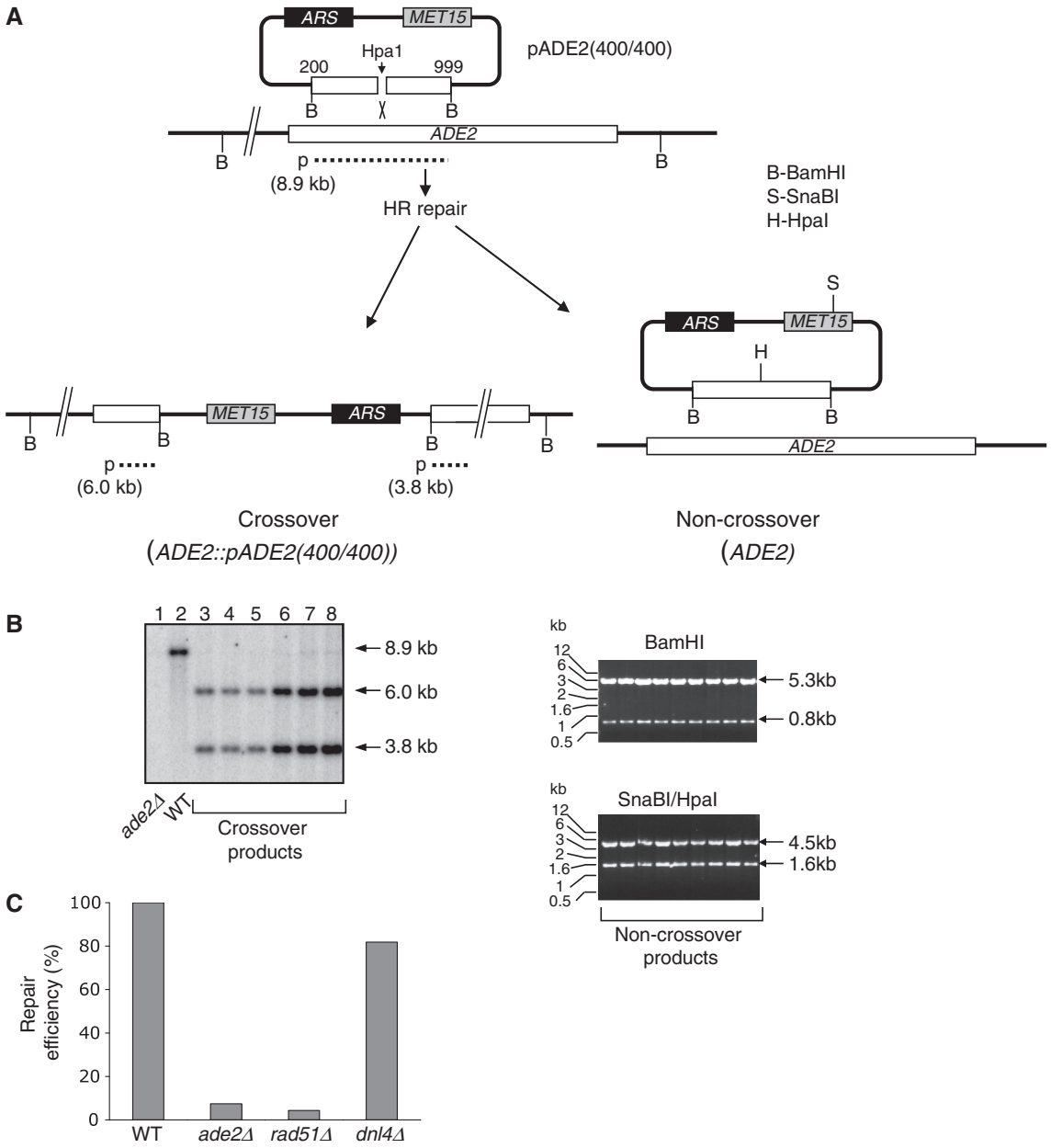

Figure 2. (**A**) Schematic diagram showing plasmid-break repair assay in which pADE2(400/400) is repaired using endogenous *ADE2* locus. HR repair of pADE2(400/400) is mediated via a 800-bp fragment comprising residues 200–999 of the *ADE2* open reading frame. pADE2(400/400) is linearized at a unique Hpa1 site which bisects the *ADE2* fragment into two 400 bp regions of homology to *ADE2*. The structures of crossover and non-crossover repair products are shown. (**B**) Confirmation of repair products. Left panel: Integration of pADE2(400/400) into the *ADE2* locus in CO events was confirmed by Southern analysis; dotted line labeled p in (A) indicates the sequence used as a probe and the sizes in parentheses indicate the predicted BamHI fragments detected in wild-type (lane 2) and six independent CO products (lanes 3–8). Shown also is genomic DNA from *ade2Δ* cells (lane 1). *Right panels*: Intact circular pADE2(400/400) plasmid was recovered from NCO products and analyzed by BamHI or SnaBI and HpaI digestion, as indicated. Predicted sizes of restriction fragments are shown on the right of each panel. (**C**) Genetic requirements for the repair of HpaI-linearized pADE2(400/400). See text for details.

(ARS) (Figure 2A). Linearization of pADE2(400/400) at a unique Hpa1 site results in 400 bp of terminal homology to *ADE2*, which is used to target the endogenous *ADE2* following transformation into yeast. Repair of pADE2 (400/400), which was assessed by selection for *MET15*, was dependent on both the endogenous *ADE2* gene and Rad51, but not Dnl4, thus confirming repair was mediated by HR and not non-homologous end-joining (Figure 2C). As predicted, CO products resulted in pADE2(400/400) integration into, and thus disruption of, the *ADE2* gene, which was confirmed by Southern analysis (Figure 2B), whereas intact circular pADE2(400/400) could be recovered from NCO products (Figure 2B). As the *ADE2* locus remained intact in NCO products, CO and NCO repair events could be visually distinguished by the red pigment that accumulates in *ade2* cells. In wild-type

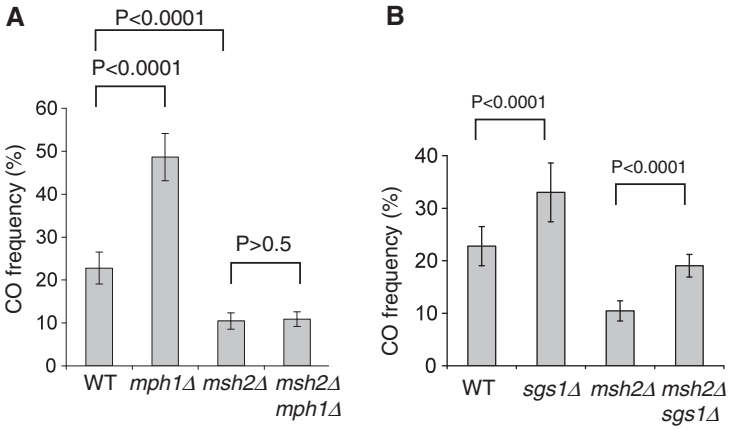

Figure 3. The anti-CO function of Mph1, but not Sgs1, requires Msh2. (**A** and **B**) CO frequency during repair of pADE2(400/400) in various genetic backgrounds, as indicated. Bars are means with standard deviations.

cells, the CO frequency for the repair of pADE2(400/400) was found to be ~20% (Figure 3A). This frequency is increased ~2-fold in *mph1Δ* cells, which is comparable to the 3-fold increase in CO formation observed during the repair of an HO endonuclease-induced genomic DSB (5). This result indicates that Mph1 functions to suppress COs during extra-chromosomal, as well as chromosomal, DSB repair (Figure 3A).

Mph1 specifically suppresses a subset of COs that are generated in a MutSα-dependent manner

To gain some insight into the mechanism by which Mph1 influences CO formation we analyzed potential genetic interactions between *MPH1* and other factors that are known to influence CO frequency. Using our assay, CO frequency is reduced 2-fold in *msh2Δ* cells, consistent with previous reports (24) (Figure 3A). However, loss of *MPH1* in an *msh2Δ* background did not result in an increase in CO formation indicating a requirement for Msh2 to generate COs that are normally suppressed by Mph1 (Figure 3A). The RecQ helicase, Sgs1, has also been shown to suppress COs during inter-chromosomal and plasmid gap HR repair (2,33,34). However, in contrast to Mph1, loss of Msh2 had no effect on the ability of Sgs1 to suppress COs (Figure 3B). This indicates that Mph1 and Sgs1 suppress distinct classes of COs that differ in their dependence on Msh2.

Next we examined which of the different functions of Msh2 are required to generate COs that are suppressed by Mph1. Loss of *MPH1* resulted in a 2–3-fold increase in CO formation in *msh3Δ* and *rad1Δ* cells (Figure 4A) indicating that the ability of Mph1 to suppress CO formation does not require the Msh3- and Rad1-dependent functions of Msh2. However, the loss of *MPH1* had no effect on the frequency of COs in *msh6Δ* cells suggesting that Mph1 suppresses COs that are generated in a MutSα-dependent manner (Figure 4A). To confirm this notion, we used a separation-of-function allele of *MSH2*, *msh2Δ1*, which contains an in-frame deletion of residues 2–133 of Msh2 (35). The *msh2Δ1* product lacks the entire mismatch recognition-binding domain 1 of Msh2 and lacks the ability to perform MutSβ-dependent MMR but is proficient for MutSα-dependent MMR (35). We mutated the endogenous *MSH2* gene to generate the *msh2Δ1* allele. Repair of pADE2(400/400) in *msh2Δ1* cells resulted in a CO frequency that was reduced compared to wild-type cells but comparable to *msh2* or *msh3* cells consistent with the *msh2Δ1* cells lacking Msh3-dependent functions of Msh2 (Figure 4A and B). However, in contrast to an *msh2Δ* background, deletion of *MPH1* in *msh2Δ1* cells resulted in a ~2-fold increase in CO frequency (Figure 4B). Together, these data indicate that during HR repair, COs are generated in a MutSα-dependent manner that are suppressed by the actions of Mph1 but not Sgs1.

The MutSα-dependent suppression of COs by Mph1 does not require the mismatch recognition function of MutSα

The observation that during repair of pADE2(400/400), Mph1 specifically suppresses COs that are MutSα-dependent was somewhat unexpected since the 800 bp *ADE2* targeting fragment in pADE2(400/400) is completely homologous to the corresponding sequence of the endogenous *ADE2* gene. Thus, Rad51-mediated strand invasion would not be expected to generate base–base mismatches, which could be recognized by MutSα. We asked therefore whether MutSα-dependent COs that are suppressed by Mph1 require the DNA mismatch recognition functions of MutSα. To do this, we replaced the endogenous *MSH6* allele with either of two different *MSH6* alleles: *msh6-340* and *msh6-G987D*. The *msh6-340* allele encodes a form of Msh6 that contains four amino acid substitutions in its mismatch recognition domain (28). As such, the Msh2-msh6-340 complex is not able to recognize mismatches but is able to bind homo-duplexes with an affinity equal to that of the wild-type Msh2–Msh6 complex. The *msh6-G987D* allele encodes a defective ATPase form of Msh6 (28,36). Msh6-G987D thus is able to recognize DNA mismatches but, unlike wild-type Msh6, remains stably bound in the presence of ATP. The ATP-dependent dissociation of MutSα from mismatch-containing DNA is thought to facilitate translocation of MutSα and the subsequent recruitment/activation

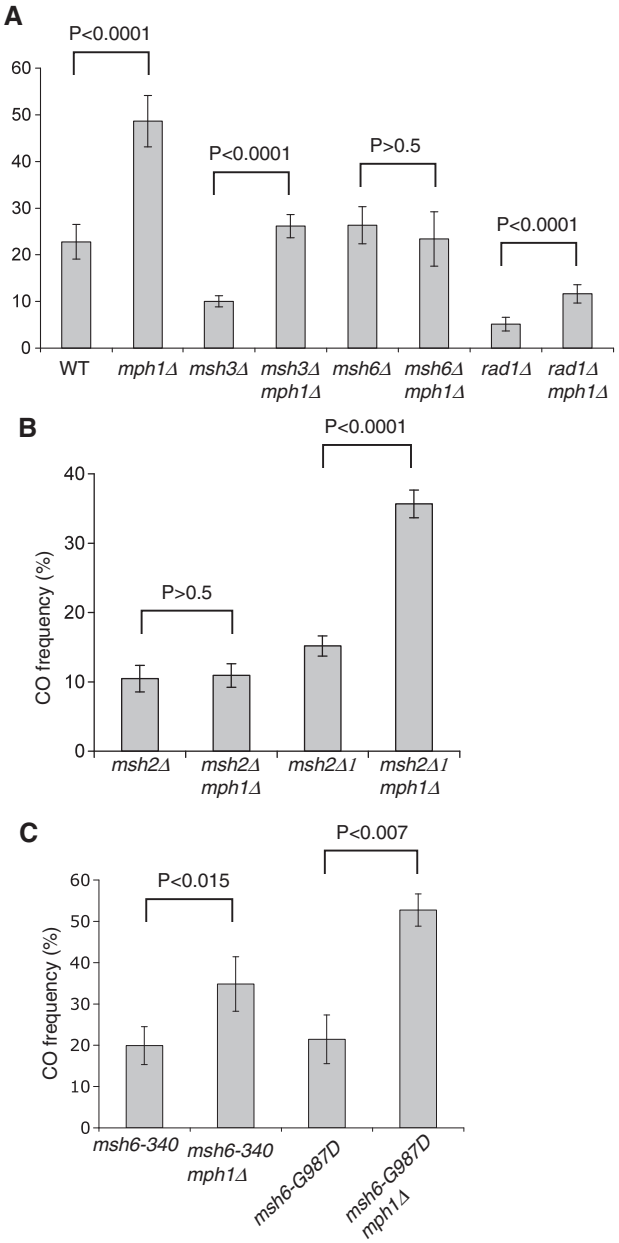

Figure 4. The anti-CO function of Mph1 is dependent on MutSα but independent of MutSβ. (**A**) CO frequency during repair of pADE2(400/400) in various genetic backgrounds, as indicated. (**B**) CO frequency during repair of pADE2(400/400) in the presence of various *msh2* alleles in the presence or absence of Mph1. (**C**) CO frequency during repair of pADE2(400/400) in the presence of various *msh6* alleles in the presence or absence of Mph1. Bars are means with standard deviations. See text for details.

of downstream MMR factors (20). Replacement of *MSH6* with either *msh6-340* or *msh6-G987D* resulted in cells having an inability to effectively recognize base–base mismatches during homeologous recombination, thus, confirming the MMR defect conferred by either allele (see below). However, a ~2-fold increase in CO frequency was observed in the absence of Mph1 in both *msh6-340* and *msh6-G987D* cells (Figure 4C). Together, these results indicate that Mph1 suppresses MutSα-dependent COs that are generated independently of the mismatch binding/processing function of MutSα.

Mph1 acts redundantly with Sgs1 to effect MutSα-dependent suppression of COs during homeologous recombination

The MMR machinery has established roles in the suppression of HR repair between homeologous sequences (14–16). Given the antagonistic relationship between Mph1 and MutSα in regulating CO formation during the repair of pADE2(400/400), we examined if Mph1 also inhibits MutSα during homeologous recombination. To do this, we introduced 10 single base changes (labeled 0–9) into the *ADE2* targeting fragment of pADE2(400/400) that were dispersed approximately every 50–60 bp to generate pADE2(1 bp/mis) (Supplementary Figure S2 and Figure 5A). pADE2(1 bp/mis) thus contained a targeting sequence that was 98.8% homologous to *ADE2*, and would be expected to generate base–base mismatches following strand invasion into the endogenous *ADE2* gene. We predicted that such mismatches will be recognized by MutSα, but not MutSβ. We confirmed this prediction by analyzing repair events in MMR mutants. Repair of pADE2(1 bp/mis) in wild-type cells resulted in a ~4-fold reduction in CO frequency when compared to the repair of pADE2(400/400) (Figure 5A). A similar magnitude of reduction in CO formation was also observed in *msh3Δ* cells whereas *msh2Δ*, *msh6Δ*, *msh6-G987D* and *msh6-340* cells were not proficient for homeology-mediated suppression of COs (Figure 5A). Together, these results confirm that homeology-mediated suppression of COs generated during the repair of pADE2(1 bp/mis) occurs in a MutSα–dependent, MutSβ-independent manner that is mediated through the base–base mismatch recognition function of MutSα (Figure 5A).

In *mph1Δ* cells, homeology-mediated suppression of COs occurred at a level that was intermediate to that of wild-type and *msh2Δ* or *msh6Δ* cells indicating that Mph1 is required to effect efficient homeology-mediated suppression of COs during the repair of pADE2(1 bp/mis) (Figure 5B). Compared to wild-type cells, *sgs1Δ* cells also showed a similar reduced ability to effect MutSα-dependent suppression of CO frequency (Figure 5B) leading us to hypothesize that Sgs1 might partially compensate for loss of Mph1 during homeology-mediated CO suppression. Indeed, the CO frequencies of pADE2(400/400) and pADE2(1 bp/mis) repair were identical in *mph1Δ sgs1Δ* double mutant cells indicating that these cells completely fail to discriminate homeologous and homologous sequences with respect to CO formation (Figure 5B). To confirm that changes in CO frequency in response to the presence of homeology are a reflection of changes in absolute CO levels, repair substrates were co-transformed with an unrelated plasmid, pYES, which contains a different auxotrophic marker, to control for transformation efficiency in order to determine absolute CO and NCO repair efficiencies. Although there was greater variation in the inter-experimental absolute repair efficiencies as compared to the CO frequencies, in

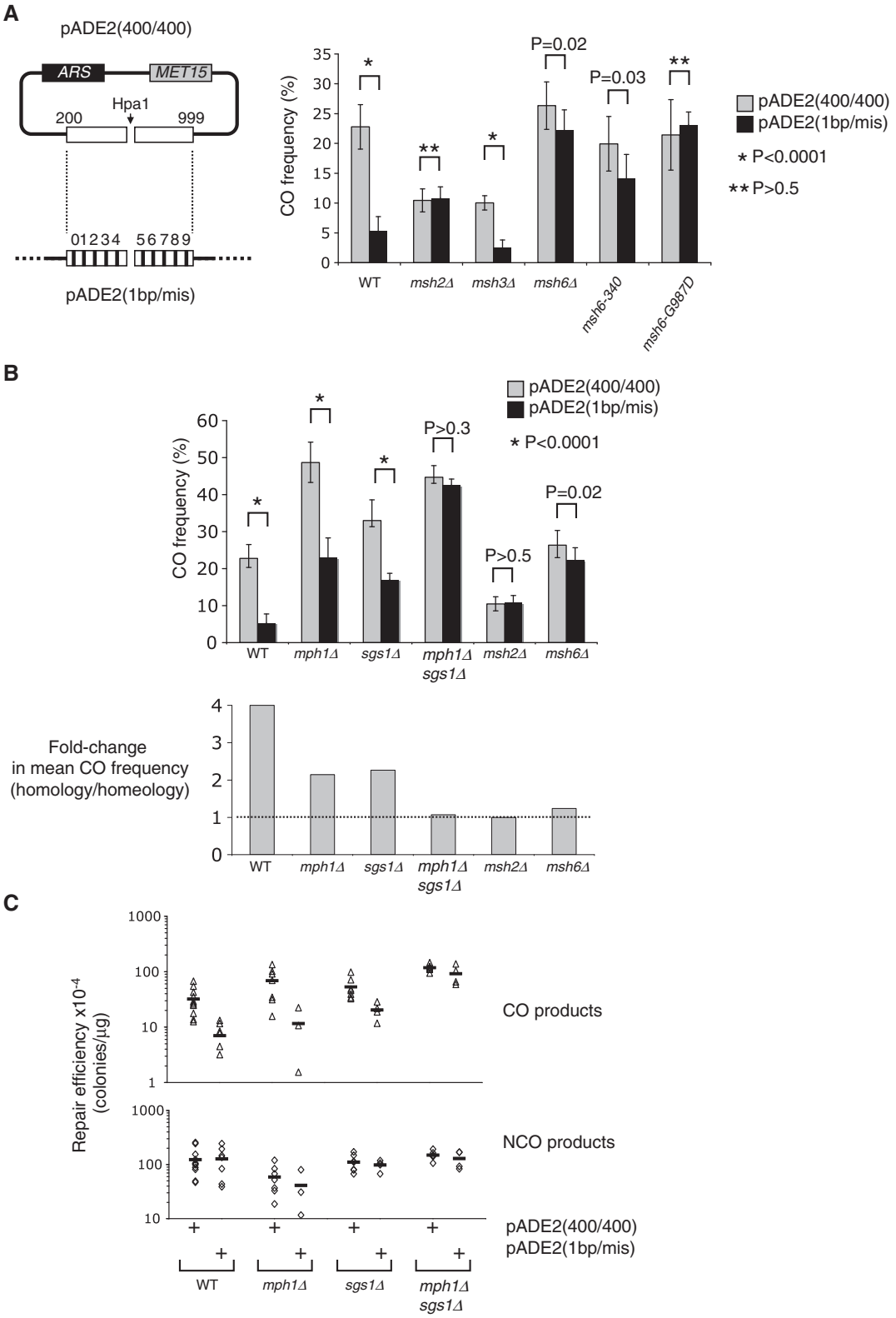

Figure 5. Homeology-mediated suppression of COs is defective in *mph1Δ sgsΔ* cells. (**A**) Left panel: Schematic diagram showing the derivation of pADE2(1 bp/mis) in which the *ADE2* targeting fragment of pADE2(400/400) has been replaced with a modified version containing 10 single base substitutions as indicated by vertical black bars. The unique HpaI site present in pADE2(400/400) is present in pADE2(1 bp/mis). *Right panel*: Comparison of CO frequencies arising from the repair of pADE2(400/400) versus pADE2(1 bp/mis) in various genetic backgrounds, as indicated. (**B**) *Upper panel*: Comparison of CO frequencies arising from the repair of pADE2(400/400) versus pADE2(1 bp/mis) in various genetic backgrounds, as indicated. *Lower panel*: Fold-change in mean CO frequencies from upper panel comparing homologous [pADE2(400/400)] and homeologous [pADE2(1bp/mis)] repair substrates. Level indicative of no-change (1-fold) is shown by a dotted line. (**C**) Absolute CO and NCO repair efficiencies following correction for transformation efficiency for repair of either pADE2(400/400) or pADE2(1 bp/mis) in different genetic backgrounds, as indicated. * indicates those datasets that share common *P*–values.

all strains tested, any differences in CO frequency between the repair of pADE2(400/400) and pADE2(1 bp/mis) were found to be due to changes in absolute CO formation. In contrast, the efficiency of NCO generation was unaffected by the presence of homeology (Figure 5C). This observation is consistent with the previous findings of Welz-Voegele *et al.* (33) who also showed that the presence of homeologous sequences has a greater inhibitory effect on CO formation. Overall, these results indicate that, together, Mph1 and Sgs1 are required for MutSα to suppress the formation of COs when homeologous sequences are utilized during HR repair.

mph1Δ sgs1Δ cells are proficient for gene conversion during homeologous recombination

Since *mph1Δ sgs1Δ* double mutant cells pheno-copy *msh2Δ* and *msh6* mutant cells in their inability to effectively discriminate homeology from homology during HR repair, this raised the possibility that the combined loss of Mph1 and Sgs1 might result in a defect in MMR (Figure 5). To analyze this possibility, we amplified by PCR the plasmid-derived *ADE2* fragments in CO and NCO products arising from the repair of pADE2(1 bp/mis) from wild-type, *mph1Δ*, *sgs1Δ*, *mph1Δ sgs1Δ* and *msh6Δ* cells using plasmid and genomic sequence specific primers (Figure 6). PCR products were sequenced to determine the GC, restoration and segregation frequency of each of the 10 individual base changes introduced into pADE2(400/400) to generate pADE2(1 bp/mis) (Figure 6 and Supplementary Figure S2). Marker segregation was used as a signature of defective MMR and occurs when the two strands of an un-repaired mismatch are segregated into daughter molecules following DNA replication, resulting in the presence of both sequences in the arising colony (37).

As expected, GC was more closely associated with CO rather than NCO events in all genetic backgrounds tested (1) (Figure 6). Marker segregation was seen in only 6% (8/140) of wild-type repair products indicating that base–base mismatch-containing DNA was efficiently disrupted by reverse branch migration or subjected to gene conversion (Figure 6). However, as predicted of a defect in MMR, 57% (27/47) of repair products from *msh6Δ* cells contained marker segregation which represented a 10-fold increase over wild-type levels (Figure 6). Tracts of marker segregation in individual repair products were also longer in CO products from *msh6Δ* cells compared to wild-type cells (Figure 6). Marker segregation tended to occur for markers 0–4, indicating an asymmetry in the processing of the two ends of the DSB (Figure 6). Despite the absence of a functional MutSα complex, *msh6Δ* cells were still able to generate significant levels of GC in CO and NCO products (Figure 6). Presumably, these GC events were mediated by Msh2/Msh3, which has partially overlapping roles with Msh2/Msh6 in recognizing base–base mismatches. Nonetheless, there is a strong correlation in *msh6Δ* cells between the levels of marker segregation and an inability to suppress COs in the presence of homeology during the repair of pADE2(1 bp/mis) (Figures 5 and 6). However, unlike *msh6Δ* cells, *mph1Δ sgs1Δ* double mutant cells did not have elevated levels of marker segregation compared to wild-type cells in either CO or NCO products (Figure 6). Together, these data indicate that the combined loss of Mph1 and Sgs1 does not result in an overt defect in DNA MMR during homeologous recombination.

NCO products that arise during homeologous recombination are processed differently in the absence of both Mph1 and Sgs1

The profile of repair products from *mph1Δ sgs1Δ* double mutant cells was however distinct from the profile of repair products from wild-type cells. Most markedly, *mph1Δ sgs1Δ* double mutant cells had elevated levels of GC in NCO products for 9 out of the 10 markers (markers 0–8) compared to wild-type NCOs (Figures 6B and 7A, lower panel). In contrast, NCO products from single mutant *mph1Δ* and *sgs1Δ* cells had GC frequencies for all 10 markers that were similar to levels found in wild-type cells (Figures 6B and 7A, lower panel). Loss of Mph1 had no effect on GC frequencies in CO products whereas loss of Sgs1 resulted in higher GC frequencies as has previously been shown (Figures 6A and 7A, upper panel) (34). This effect, however, was only observed for markers 5–9 consistent with the observed asymmetry in which the two ends of the DSB are processed in *msh6Δ* cells (Figure 7A, upper panel). These results indicate that while Sgs1 suppresses GC in both CO and NCO products, Mph1 specifically acts to suppress GC in NCO products and does so in a redundant manner with Sgs1.

The profile of GC tract directionality was also altered in *mph1Δ sgs1Δ* double mutant cells compared to wild-type cells (Figure 7B). The proportion of repair products containing uni- and bi-directional GC tracts in NCOs was similar between wild-type and single mutant *mph1Δ* and *sgs1Δ* cells (Figure 7B, lower panel). However, there was a 10-fold increase in bi-directional GC tracts in *mph1Δ sgs1Δ* double mutant cells compared to wild-type cells or the single mutant *mph1Δ* and *sgs1Δ* cells at the expense of repair events showing no GC (Figure 7B, lower panel). In contrast, Mph1 had no effect on the proportion of uni- and bi-directional GC tracts of CO products either in the presence of absence of Sgs1 whereas loss of Sgs1 resulted in an increase in bi-directional GC tracts (Figure 7B, upper panel). Together, these results indicate that, during homeologous recombination repair, NCOs are processed differently in the absence of both Mph1 and Sgs1, giving rise to increases in GC tract length and bi-directional GC tracts.

DISCUSSION

The suppression of COs during HR repair is imperative for the prevention of deleterious genomic rearrangements when non-sisters recombine. The DNA helicase Mph1 has been shown to negatively regulate the formation of COs during HR repair of a genomic DSB (4). Here, we have confirmed this function of Mph1 in a plasmid break repair assay, indicating that Mph1 plays a core role in regulating CO formation during both chromosomal and extra chromosomal HR repair. Consistent with this notion is the

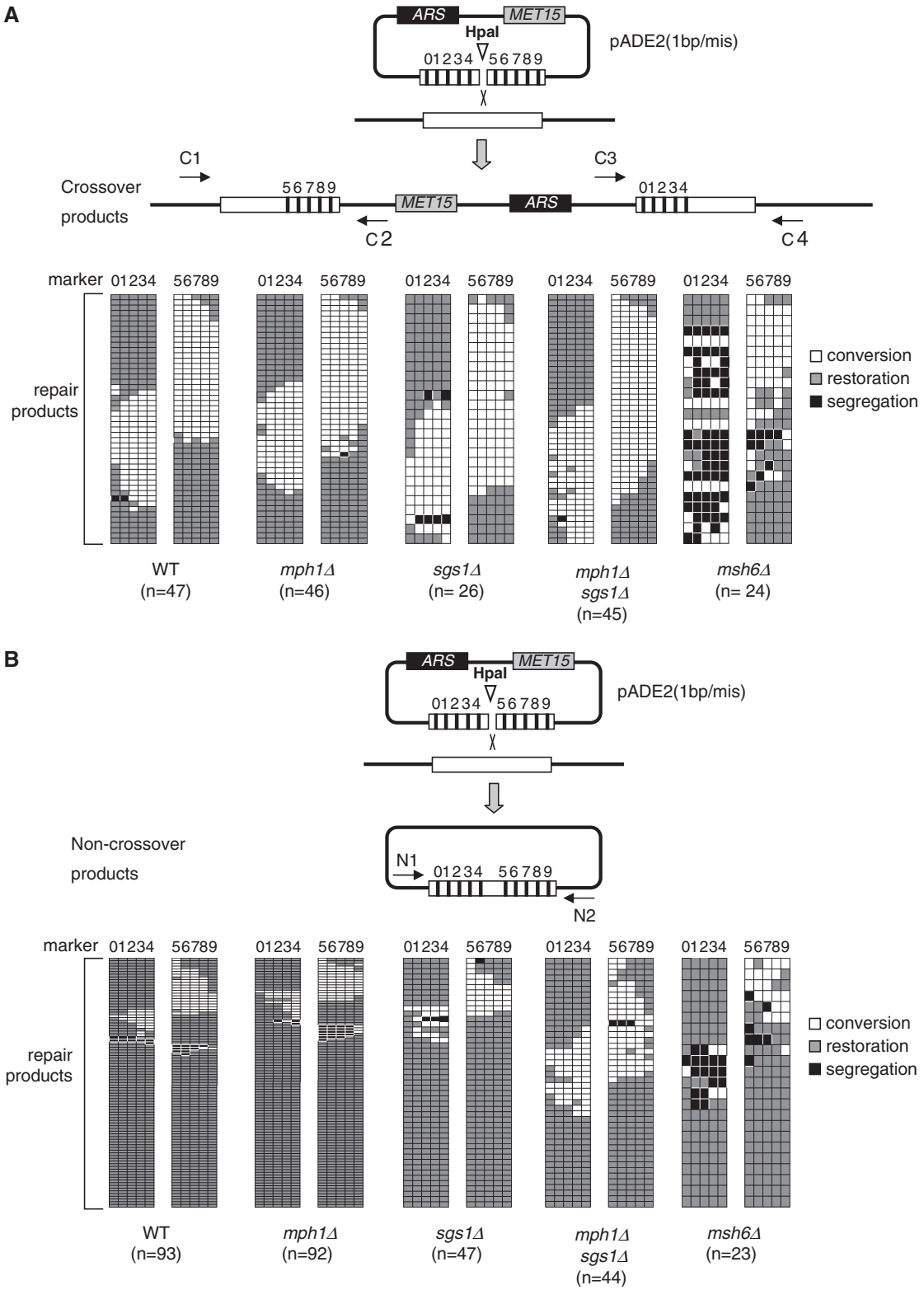

Figure 6. *mph1Δ sgs1Δ* cells do not have an overt defect in mismatch recognition but display altered processing of non-crossover products. (**A**) Upper panel: Schematic diagram showing the formation of CO products resulting from the repair of pADE2(1 bp/mis). The positions of single bases (labeled 0–9) differing from the wild-type *ADE2* sequence are indicated by vertical black lines. The location of the HpaI-induced break is indicated by an open arrowhead. Black arrows indicate primers used to amplify by PCR the indicated fragments from CO products for marker analysis. Lower panel: Status of each of the markers 0–9 in individual repair products from different genetic backgrounds, as indicated. Number of individual repair products analyzed from each genetic background is shown in parentheses. (**B**) Upper panel: Schematic diagram showing the formation of NCO products resulting from the repair of pADE2(1 bp/mis). The position of single bases (labeled 0–9) differing from the wild-type *ADE2* sequence are indicated by vertical black lines. The location of the HpaI-induced break is indicated by an open arrowhead. Black arrows indicate primers used to amplify by PCR the indicated fragment from NCO products for marker analysis. Lower panel: Status of each of the markers 0–9 in individual repair products from different genetic backgrounds, as indicated. Number of individual repair products analyzed from each genetic background is shown in parentheses. To aid comparison between strains in (A) and (B), the data for each strain has been proportionally scaled in order that the total number of repair products occupy the same area.

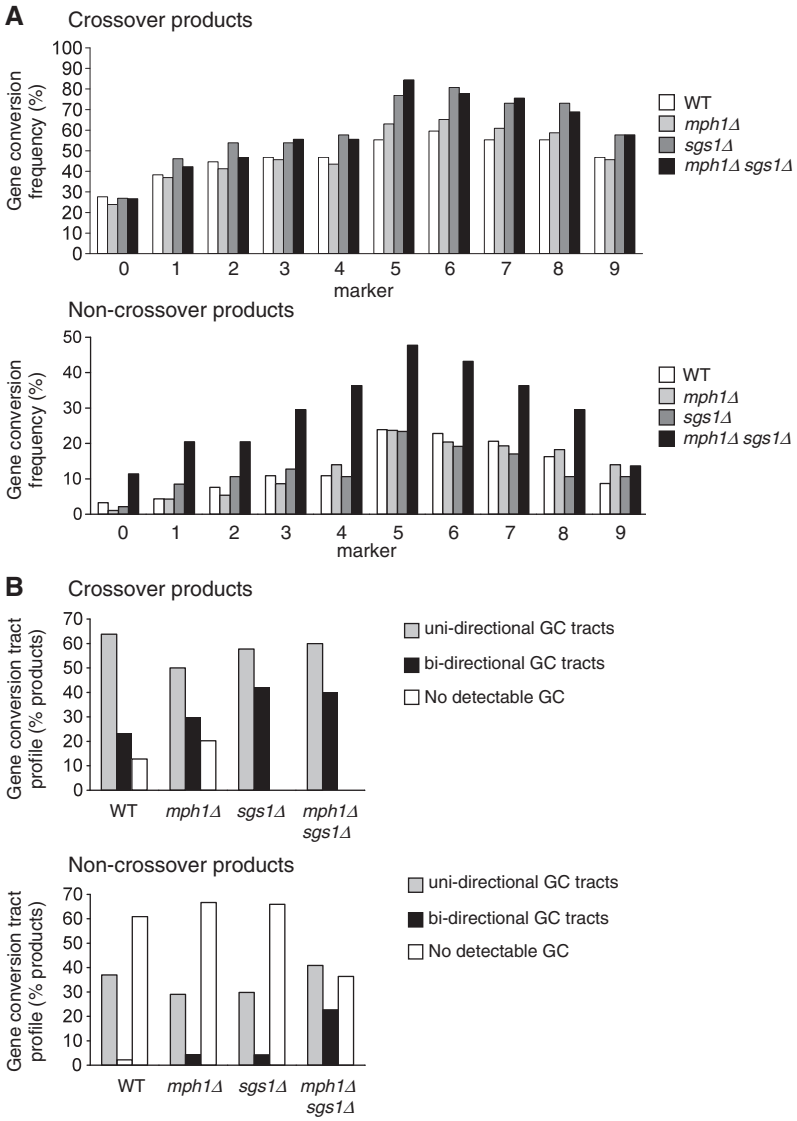

Figure 7. Non-crossover products from *mph1Δ sgs1Δ* cells have elevated frequencies of gene conversion and bi-directional gene conversion tracts. (**A**) Upper panel: Gene conversion frequencies for individual markers 0–9 in CO products resulting from the repair of pADE2(1 bp/mis) in various genetic backgrounds, as determined from Figure 6A. Lower panel: Gene conversion frequencies for individual markers 0–9 in NCO products resulting from the repair of pADE2(1 bp/mis) in various genetic backgrounds, as determined from Figure 6B. (**B**) Upper panel: Gene conversion tract directionality of CO products resulting from the repair of pADE2(1 bp/mis) in various genetic backgrounds, as determined from Figure 6A. Lower panel: Gene conversion tract directionality of NCO products resulting from the repair of pADE2(1 bp/mis) in various genetic backgrounds, as determined from Figure 6B.

ability of the *S. pombe* Mph1 homolog, Fml1, to suppress CO formation in a plasmid gap repair assay (38). Moreover, we have shown that the anti-CO function of Mph1 is absolutely dependent on MutSα. Previous studies have implicated MutSβ, but not MutSα, in the formation of COs during inter-chromosomal recombination (24,25). However, our results indicate that during HR repair, a subset of COs are indeed generated in a MutSα-dependent manner but that the formation of these COs is antagonized by the actions of Mph1. This would explain why losing Msh6 alone has no effect on CO frequency since MutSα-dependent COs will normally be suppressed in wild-type cells by Mph1 (Figure 4A). In contrast, Sgs1 did not suppress MutSα-dependent COs. Sgs1 has been shown to cooperate with MutSα in other forms of HR repair such as SSA, indicating HR pathway-specific interactions between Mph1, Sgs1 and MutSα (39). MutSα-dependent COs that are suppressed by Mph1 do not require the presence of sequence divergence between the recombining sequences or, indeed, the mismatch recognition function of MutSα (Figure 4C). This suggests that Mph1 is recruited to HR intermediates through a constitutive function of MutSα. Consistent with this idea is the finding that Mph1 and Msh6 are found to physically interact in undamaged cells (40).

In contrast to the antagonistic interaction observed between Mph1 and MutSα when a completely homologous sequence was used to target repair, Mph1, together

with Sgs1, was required for the efficient MutSα-dependent suppression of COs during homeologous recombination repair of pADE2 (1 bp/mis) (Figure 5). This observation is consistent with recent findings that show Mph1 and Sgs1 can suppress chromosomal rearrangements mediated through non-allelic homeologous loci (41). As expected, CO suppression during pADE2 (1 bp/mis) repair required the MMR functions of MutSα. However, our results did not reveal an overt defect in MMR in *mph1Δ sgs1Δ* double mutant cells but rather indicated that in the absence of both Mph1 and Sgs1, NCOs are generated differently to when either or both helicases are present (Figures 6 and 7). NCOs generated by SDSA or double HJ dissolution tend to have short or undetectable GC tracts. This is because SDSA and dissolution require the disruption of D-loops and convergent double HJ branch migration, respectively, which limits the length of heteroduplex DNA and thus reduces the potential for mismatches distal to the break initiating MMR and causing GC (Figure 1). Conversely, NCOs generated by HJ resolution would be expected to have the GC profile of CO products, as the two products result simply from HJ resolution occurring in alternative orientations (Figure 1). The finding that the GC profile of NCOs was unaffected in *mph1Δ* and *sgs1Δ* cells supports the notion that, in the absence of Mph1 or Sgs1, which results in compromised SDSA and dissolution, respectively, the majority of NCOs are generated by the remaining, intact NCO pathway. However, the altered GC profile of NCOs from *mph1Δ sgs1Δ* double mutant cells compared to wild-type or single mutant *mph1Δ* and *sgs1Δ* cells is consistent with a higher proportion of NCO products generated via HJ resolution. We also found that Mph1 had no effect on GC in CO products whereas the loss of Sgs1 gave rise to an increase in GC, as has previously been reported (34). This observation is wholly consistent with a role for Mph1 in SDSA, because, in the absence of SDSA the channeling of intermediates into dissolution/resolution pathways of HR would be expected to affect the quantity of COs but not the GC profile of COs (Figure 1). These results thus provide *in vivo* evidence to support the proposed roles for Mph1 and Sgs1 in SDSA and dissolution, respectively and support the notion that, in mitotic HR repair, HJ resolution predominantly occurs as a back-up pathway when SDSA and dissolution are attenuated.

In conclusion, we have shown that the anti-CO functions of Mph1 are intricately linked to the MMR factor MutSα. A model outlining how we propose Mph1, Sgs1 and MutSα interact to regulate CO formation during homologous and homeologous recombination is shown in Figure 1. The nature of these interactions is highly dependent on the nature of the recombining sequences since MutSα can promote (in the presence of homologous sequences) or suppress (in the presence of homeologous sequences) the formation of COs during the HR repair of DSBs. We propose that this latter role of MutSα, which requires its MMR function, acts to suppress the formation of double HJs during homeologous recombination by acting on the increased tracts of mismatches that are generated through Rad51-mediated D-loop extension and second end capture (Figure 1, yellow box). Mph1 may thus promote MutSα-dependent suppression of double HJ formation by its ability to disrupt D-loops, thus circumventing the generation of mismatches. This proposal would explain why Mph1 is required for MutSα-dependent homeology-mediated suppression of COs without itself being a core component of the MMR machinery (Figure 1) (4,9). In contrast, we propose that the MMR-independent functions of MutSα are required for the processing of double HJs into CO products and that this step is specifically inhibited by Mph1 but not Sgs1 (Figure 1, green box). Our results therefore suggest that MutSα has multiple, separable functions in MMR and HR. Such a situation exists for MutSβ whereby mutant alleles of *MSH2* indicate that the removal of non-homologous tails, and, heteroduplex rejection during SSA, are separable functions of MutSβ (42). In addition to having a binding preference for mismatch-containing DNA, MutSα also binds HO-induced DSBs and synthetic HJs (43–45). Such activities may be relevant to the pro-crossover function of MutSα during HR repair of DSBs and could be reminiscent of the function of the MSH4/MSH5 complex, which does not have a role in MMR but can bind HJs and has pro-crossover functions during meiosis (46–48). How Msh6 performs functions aside from its role in mismatch recognition, and the molecular basis of how Mph1 and MutSα might cooperate to recognize and process recombination intermediates that do not contain base–base mismatches, are currently under investigation.

Mutations in the human homologues of Mph1, Msh2, Msh6 and Sgs1 (FANCM, hMSH2, hMSH6 and BLM, respectively) give rise to cancer-prone disorders that are associated with aberrant HR and genome instability (49–56). Our findings, which were derived in haploid strains of *S. cerevisiae*, are likely to be highly relevant to human cells where the potential for ectopic recombination and thus the necessity to suppress CO formation will be greater given the diploid and repetitive nature of the human genome.

SUPPLEMENTARY DATA

Supplementary Data are available at NAR Online.

ACKNOWLEDGEMENTS

The authors thank Eric Alani and Francesca Storici for kind gifts of plasmids, Ian Hickson and Peter McHugh for the *mph1Δ sgs1Δ* strain and helpful comments on the manuscript, and members of the Chromosome Stability Group for useful discussions.

FUNDING

This work was funded by Cancer Research UK.

Conflict of interest statement. None declared.

REFERENCE

1. Paques,F. and Haber,J.E. (1999) Multiple pathways of recombination induced by double-strand breaks in Saccharomyces cerevisiae. *Microbiol. Mol. Biol. Rev.*, **63**, 349–404.
2. Ira,G., Malkova,A., Liberi,G., Foiani,M. and Haber,J.E. (2003) Srs2 and Sgs1-Top3 suppress crossovers during double-strand break repair in yeast. *Cell*, **115**, 401–411.
3. Wu,L. and Hickson,I.D. (2003) The Bloom's syndrome helicase suppresses crossing over during homologous recombination. *Nature*, **426**, 870–874.
4. Prakash,R., Satory,D., Dray,E., Papusha,A., Scheller,J., Kramer,W., Krejci,L., Klein,H., Haber,J.E., Sung,P. *et al.* (2009) Yeast Mph1 helicase dissociates Rad51-made D-loops: implications for crossover control in mitotic recombination. *Genes Dev.*, **23**, 67–79.
5. Kang,Y.H., Kang,M.J., Kim,J.H., Lee,C.H., Cho,I.T., Hurwitz,J. and Seo,Y.S. (2009) The MPH1 gene of Saccharomyces cerevisiae functions in Okazaki fragment processing. *J. Biol. Chem.*, **284**, 10376–10386.
6. St Onge,R.P., Mani,R., Oh,J., Proctor,M., Fung,E., Davis,R.W., Nislow,C., Roth,F.P. and Giaever,G. (2007) Systematic pathway analysis using high-resolution fitness profiling of combinatorial gene deletions. *Nat. Genet.*, **39**, 199–206.
7. Prakash,R., Krejci,L., Van Komen,S., Anke Schurer,K., Kramer,W. and Sung,P. (2005) Saccharomyces cerevisiae MPH1 gene, required for homologous recombination-mediated mutation avoidance, encodes a 3′ to 5′ DNA helicase. *J. Biol. Chem.*, **280**, 7854–7860.
8. Schurer,K.A., Rudolph,C., Ulrich,H.D. and Kramer,W. (2004) Yeast MPH1 gene functions in an error-free DNA damage bypass pathway that requires genes from Homologous recombination, but not from postreplicative repair. *Genetics*, **166**, 1673–1686.
9. Scheller,J., Schurer,A., Rudolph,C., Hettwer,S. and Kramer,W. (2000) MPH1, a yeast gene encoding a DEAH protein, plays a role in protection of the genome from spontaneous and chemically induced damage. *Genetics*, **155**, 1069–1081.
10. Chang,M., Bellaoui,M., Zhang,C., Desai,R., Morozov,P., Delgado-Cruzata,L., Rothstein,R., Freyer,G.A., Boone,C. and Brown,G.W. (2005) RMI1/NCE4, a suppressor of genome instability, encodes a member of the RecQ helicase/Topo III complex. *EMBO J.*, **24**, 2024–2033.
11. Krejci,L., Van Komen,S., Li,Y., Villemain,J., Reddy,M.S., Klein,H., Ellenberger,T. and Sung,P. (2003) DNA helicase Srs2 disrupts the Rad51 presynaptic filament. *Nature*, **423**, 305–309.
12. Mullen,J.R., Nallaseth,F.S., Lan,Y.Q., Slagle,C.E. and Brill,S.J. (2005) Yeast Rmi1/Nce4 controls genome stability as a subunit of the Sgs1-Top3 complex. *Mol. Cell Biol.*, **25**, 4476–4487.
13. Veaute,X., Jeusset,J., Soustelle,C., Kowalczykowski,S.C., Le Cam,E. and Fabre,F. (2003) The Srs2 helicase prevents recombination by disrupting Rad51 nucleoprotein filaments. *Nature*, **423**, 309–312.
14. Bailis,A.M. and Rothstein,R. (1990) A defect in mismatch repair in Saccharomyces cerevisiae stimulates ectopic recombination between homeologous genes by an excision repair dependent process. *Genetics*, **126**, 535–547.
15. Datta,A., Adjiri,A., New,L., Crouse,G.F. and Jinks Robertson,S. (1996) Mitotic crossovers between diverged sequences are regulated by mismatch repair proteins in Saccaromyces cerevisiae. *Mol. Cell Biol.*, **16**, 1085–1093.
16. Selva,E.M., New,L., Crouse,G.F. and Lahue,R.S. (1995) Mismatch correction acts as a barrier to homeologous recombination in Saccharomyces cerevisiae. *Genetics*, **139**, 1175–1188.
17. Harfe,B.D. and Jinks-Robertson,S. (2000) DNA mismatch repair and genetic instability. *Annu. Rev. Genet.*, **34**, 359–399.
18. Jiricny,J. (2006) The multifaceted mismatch-repair system. *Nat. Rev. Mol. Cell Biol.*, **7**, 335–346.
19. Kolodner,R. (1996) Biochemistry and genetics of eukaryotic mismatch repair. *Genes Dev.*, **10**, 1433–1442.
20. Surtees,J.A., Argueso,J.L. and Alani,E. (2004) Mismatch repair proteins: key regulators of genetic recombination. *Cytogenet. Genome Res.*, **107**, 146–159.
21. Paques,F. and Haber,J.E. (1997) Two pathways for removal of nonhomologous DNA ends during double-strand break repair in Saccharomyces cerevisiae. *Mol. Cell Biol.*, **17**, 6765–6771.
22. Fishman-Lobell,J. and Haber,J.E. (1992) Removal of nonhomologous DNA ends in double-strand break recombination: the role of the yeast ultraviolet repair gene RAD1. *Science*, **258**, 480–484.
23. Sugawara,N., Paques,F., Colaiacovo,M. and Haber,J.E. (1997) Role of Saccharomyces cerevisiae Msh2 and Msh3 repair proteins in double-strand break-induced recombination. *Proc. Natl Acad. Sci. USA*, **94**, 9214–9219.
24. Nicholson,A., Fabbri,R.M., Reeves,J.W. and Crouse,G.F. (2006) The effects of mismatch repair and RAD1 genes on interchromosomal crossover recombination in Saccharomyces cerevisiae. *Genetics*, **173**, 647–659.
25. Saparbaev,M., Prakash,L. and Prakash,S. (1996) Requirement of mismatch repair genes MSH2 and MSH3 in the RAD1-RAD10 pathway of mitotic recombination in Saccharomyces cerevisiae. *Genetics*, **142**, 727–736.
26. Symington,L.S., Kang,L.E. and Moreau,S. (2000) Alteration of gene conversion tract length and associated crossing over during plasmid gap repair in nuclease-deficient strains of Saccharomyces cerevisiae. *Nucleic Acids Res.*, **28**, 4649–4656.
27. Storici,F. and Resnick,M.A. (2006) The delitto perfetto approach to in vivo site-directed mutagenesis and chromosome rearrangements with synthetic oligonucleotides in yeast. *Methods Enzymol.*, **409**, 329–345.
28. Bowers,J., Tran,P.T., Liskay,R.M. and Alani,E. (2000) Analysis of yeast MSH2-MSH6 suggests that the initiation of mismatch repair can be separated into discrete steps. *J. Mol. Biol.*, **302**, 327–338.
29. Studamire,B., Quach,T. and Alani,E. (1998) Saccharomyces cerevisiae Msh2p and Msh6p ATPase activities are both required during mismatch repair. *Mol. Cell Biol.*, **18**, 7590–7601.
30. Szostak,J.W., Orr-Weaver,T.L., Rothstein,R.J. and Stahl,F.W. (1983) The double-strand-break repair model for recombination. *Cell*, **33**, 25–35.
31. Bartsch,S., Kang,L.E. and Symington,L.S. (2000) RAD51 is required for the repair of plasmid double-stranded DNA gaps from either plasmid or chromosomal templates. *Mol. Cell Biol.*, **20**, 1194–1205.
32. Symington,L.S. (2002) Role of RAD52 epistasis group genes in homologous recombination and double-strand break repair. *Microbiol. Mol. Biol. Rev.*, **66**, 630–670, table of contents.
33. Welz-Voegele,C. and Jinks-Robertson,S. (2008) Sequence divergence impedes crossover more than noncrossover events during mitotic gap repair in yeast. *Genetics*, **179**, 1251–1262.
34. Lo,Y.C., Paffett,K.S., Amit,O., Clikeman,J.A., Sterk,R., Brenneman,M.A. and Nickoloff,J.A. (2006) Sgs1 regulates gene conversion tract lengths and crossovers independently of its helicase activity. *Mol. Cell Biol.*, **26**, 4086–4094.
35. Lee,S.D., Surtees,J.A. and Alani,E. (2007) Saccharomyces cerevisiae MSH2-MSH3 and MSH2-MSH6 complexes display distinct requirements for DNA binding domain I in mismatch recognition. *J. Mol. Biol.*, **366**, 53–66.
36. Bowers,J., Sokolsky,T., Quach,T. and Alani,E. (1999) A mutation in the MSH6 subunit of the Saccharomyces cerevisiae MSH2-MSH6 complex disrupts mismatch recognition. *J. Biol. Chem.*, **274**, 16115–16125.
37. White,J.H., Lusnak,K. and Fogel,S. (1985) Mismatch-specific post-meiotic segregation frequency in yeast suggests a heteroduplex recombination intermediate. *Nature*, **315**, 350–352.
38. Sun,W., Nandi,S., Osman,F., Ahn,J.S., Jakovleska,J., Lorenz,A. and Whitby,M.C. (2008) The FANCM ortholog Fml1 promotes recombination at stalled replication forks and limits crossing over during DNA double-strand break repair. *Mol. Cell*, **32**, 118–128.
39. Sugawara,N., Goldfarb,T., Studamire,B., Alani,E. and Haber,J.E. (2004) Heteroduplex rejection during single-strand annealing requires Sgs1 helicase and mismatch repair proteins Msh2 and Msh6 but not Pms1. *Proc. Natl Acad. Sci. USA*, **101**, 9315–9320.
40. Gavin,A.C., Bosche,M., Krause,R., Grandi,P., Marzioch,M., Bauer,A., Schultz,J., Rick,J.M., Michon,A.M., Cruciat,C.M. *et al.* (2002) Functional organization of the yeast proteome by systematic analysis of protein complexes. *Nature*, **415**, 141–147.

41. Putnam,C.D., Hayes,T.K. and Kolodner,R.D. (2009) Specific pathways prevent duplication-mediated genome rearrangements. *Nature*, **460**, 984–989.
42. Goldfarb,T. and Alani,E. (2005) Distinct roles for the Saccharomyces cerevisiae mismatch repair proteins in heteroduplex rejection, mismatch repair and nonhomologous tail removal. *Genetics*, **169**, 563–574.
43. Alani,E., Lee,S., Kane,M.F., Griffith,J. and Kolodner,R.D. (1997) Saccharomyces cerevisiae MSH2, a mispaired base recognition protein, also recognizes Holliday junctions in DNA. *J. Mol. Biol.*, **265**, 289–301.
44. Lyndaker,A.M., Goldfarb,T. and Alani,E. (2008) Mutants defective in Rad1-Rad10-Slx4 exhibit a unique pattern of viability during mating-type switching in Saccharomyces cerevisiae. *Genetics*, **179**, 1807–1821.
45. Marsischky,G.T., Lee,S., Griffith,J. and Kolodner,R.D. (1999) 'Saccharomyces cerevisiae MSH2/6 complex interacts with Holliday junctions and facilitates their cleavage by phage resolution enzymes. *J. Biol. Chem.*, **274**, 7200–7206.
46. Hollingsworth,N.M., Ponte,L. and Halsey,C. (1995) MSH5, a novel MutS homolog, facilitates meiotic reciprocal recombination between homologs in Saccharomyces cerevisiae but not mismatch repair. *Genes Dev.*, **9**, 1728–1739.
47. Ross-Macdonald,P. and Roeder,G.S. (1994) Mutation of a meiosis-specific MutS homolog decreases crossing over but not mismatch correction. *Cell*, **79**, 1069–1080.
48. Snowden,T., Acharya,S., Butz,C., Berardini,M. and Fishel,R. (2004) hMSH4-hMSH5 recognizes Holliday Junctions and forms a meiosis-specific sliding clamp that embraces homologous chromosomes. *Mol. Cell*, **15**, 437–451.
49. Bakker,S.T., van de Vrugt,H.J., Rooimans,M.A., Oostra,A.B., Steltenpool,J., Delzenne-Goette,E., van der Wal,A., van der Valk,M., Joenje,H., Te Riele,H. *et al.* (2009) Fancm-deficient mice reveal unique features of Fanconi anemia complementation group M. *Hum. Mol. Genet.*, **18**, 3484–3495.
50. Chaganti,R.S., Schonberg,S. and German,J. (1974) A manyfold increase in sister chromatid exchanges in Bloom's syndrome lymphocytes. *Proc. Natl Acad. Sci. USA*, **71**, 4508–4512.
51. Ellis,N.A., Groden,J., Ye,T.Z., Straughen,J., Lennon,D.J., Ciocci,S., Proytcheva,M. and German,J. (1995) The Bloom's syndrome gene product is homologous to RecQ helicases. *Cell*, **83**, 655–666.
52. Fishel,R., Lescoe,M.K., Rao,M.R., Copeland,N.G., Jenkins,N.A., Garber,J., Kane,M. and Kolodner,R. (1993) The human mutator gene homolog MSH2 and its association with hereditary nonpolyposis colon cancer. *Cell*, **75**, 1027–038.
53. Leach,F.S., Nicolaides,N.C., Papadopoulos,N., Liu,B., Jen,J., Parsons,R., Peltomaki,P., Sistonen,P., Aaltonen,L.A., Nystrom-Lahti,M. *et al.* (1993) Mutations of a mutS homolog in hereditary nonpolyposis colorectal cancer. *Cell*, **75**, 1215–1225.
54. Miyaki,M., Konishi,M., Tanaka,K., Kikuchi-Yanoshita,R., Muraoka,M., Yasuno,M., Igari,T., Koike,M., Chiba,M. and Mori,T. (1997) Germline mutation of MSH6 as the cause of hereditary nonpolyposis colorectal cancer. *Nat. Genet.*, **17**, 271–272.
55. Mosedale,G., Niedzwiedz,W., Alpi,A., Perrina,F., Pereira-Leal,J.B., Johnson,M., Langevin,F., Pace,P. and Patel,K.J. (2005) The vertebrate Hef ortholog is a component of the Fanconi anemia tumor-suppressor pathway. *Nat. Struct. Mol. Biol.*, **12**, 763–771.
56. Rosado,I.V., Niedzwiedz,W., Alpi,A.F. and Patel,K.J. (2009) The Walker B motif in avian FANCM is required to limit sister chromatid exchanges but is dispensable for DNA crosslink repair. *Nucleic Acids Res.*, **37**, 4360–4370.